Further determinations of strong scintillation effects on GNSS signals using the Hybrid Scintillation Propagation Model

Nikolay N. Zernov,[1] Vadim E. Gherm,[1] and Hal J. Strangeways[2]

Received 24 November 2011; revised 20 February 2012; accepted 1 March 2012; published 17 April 2012.

[1] The effect of strong scintillation conditions on GNSS transionospheric paths of propagation is further investigated employing the most recent update of the Hybrid Scintillation Propagation Model (HSPM). The variation of various parameters including spectral indices and other statistical moments of the field is studied as a function of the severity of the signal fluctuations. The correlation time of the complex amplitude of the field is found to rapidly decrease as the scintillation severity increases, but by contrast, the intensity correlation time stays almost constant over a wide range of S_4 showing only slight decrease in the model's range of validity. The dependence of the spectral indices of both phase and amplitude on S_4 is also determined, and the spectral index of the phase fluctuations tends to 2 for the most severe scintillation, as expected from both experiment and theory. The effect of "canonical fading" is also studied, when, in the conditions of strong scintillation, fast phase changes occur along with deep amplitude fades. The probability of the effect of the "canonical fading" is studied for the conditions of strong scintillation, and the mean time between cycle slips shows a significant decrease as S_4 increases. A comparison is also presented between calculated results of S_4, spectral indices, and the correlation radii of the complex field and field intensity, utilizing both the HPSM and equivalent phase screen model for both weak and strong scintillation conditions. These show the differences that can occur which can also depend on the equivalent phase screen height.

Citation: Zernov, N. N., V. E. Gherm, and H. J. Strangeways (2012), Further determinations of strong scintillation effects on GNSS signals using the Hybrid Scintillation Propagation Model, *Radio Sci.*, *47*, RS0L06, doi:10.1029/2011RS004935.

1. Introduction

[2] Numerous effects of GNSS signal scintillations on transionospheric paths of propagation have been studied employing the St. Petersburg-Leeds-Newcastle Hybrid Scintillation Propagation Model. The initial version of the model [*Gherm et al.*, 2000] was solely based on Rytov's approximation and was therefore limited to weak and moderate scintillation conditions. To account for the case of strong scintillation, it was further extended as a combination of Rytov's method and the classical random screen technique [*Gherm et al.*, 2005]. The extended model was termed the Hybrid Scintillation Propagation Model (HSPM).

[3] Various scenarios of propagation have been studied utilizing the HSPM. In particular, in the work by *Maurits et al.* [2008] some typical properties of scintillations relevant to transionospheric paths of propagation at high latitudes have been studied including that from polar patches. In this case the University of Alaska Fairbanks Eulerian Parallel Polar Ionosphere Model was used to model the background high-latitude ionosphere. *Zernov et al.* [2009] also investigated the scintillation effects due to the bubbles occurring in the equatorial ionosphere. In this paper a very good agreement of the model results with the experimental data was reported in modeling the time dependence of the scintillation index S_4 as a group of bubbles traversed the signal paths from two satellites of the GPS constellation to a receiver at the Earth's surface in Cameroon. The most recent update of the HSPM [*Gherm et al.*, 2011a] enabled investigation of the scintillation effects of the GNNS signals at two different frequencies (as for the dual-frequency mode of operation) for the same satellite to receiver path. In particular, the effects of correlation/decorrelation of the field phases at different frequencies were studied, and the contribution of the diffraction into the range error in the dual-frequency method was assessed. To allow for the description of the two-frequency effects, the state-of-the-art version of the HSPM was developed, which, when generating the two physical random screens and then determining the appropriate times series of the fields, also takes into account the effects of mutual correlation of the fields at the different frequencies.

[4] In the present paper, we further employ the HSPM in order to address a number of the effects of scintillation on GNSS signals for transionospheric paths of propagation, specifically, for the case of strong scintillation. In section 2

[1]Department of Radio Physics, University of St. Petersburg, St. Petersburg, Russia.
[2]School of Electrical, Electronic and Computer Engineering, University of Newcastle, Newcastle upon Tyne, UK.

0048-6604/12/2011RS004935

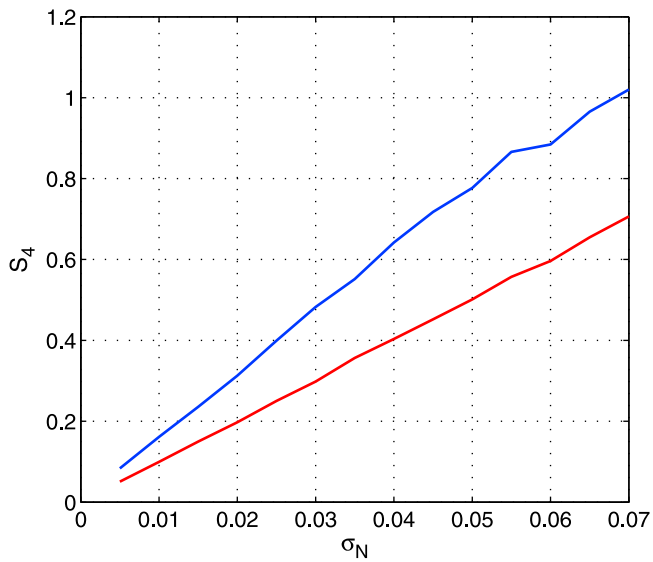

Figure 1. Scintillation index S_4 on the screen below the ionosphere (red) and on the Earth's surface (blue) as a function of the variance of the ionospheric fractional electron density σ_N^2.

the dependence of a number of the indices and other statistical moments of scintillation of the transionospheric field are studied as a function of the severity of the signal fluctuations. These include the time correlation radius of the field intensity, τ_I and of the complex amplitude of the random field τ_C and the spectral indices of the phase and log amplitude fluctuations (p_a and p_ϕ, respectively).

[5] In section 3 the effect of the full cycle phase accumulation is considered. In the conditions of strong scintillation, the deep amplitude fades frequently occur. This is likely to be accompanied by fast phase changes, which may lead to full $2\pi M$ radians (where M is a positive, or negative integer) phase accumulation. The probability of this effect is studied for the conditions of strong scintillation.

[6] Finally, section 4 is devoted to a discussion of the problem of the consistency/inconsistency of the equivalent phase screen model for the interpretation of the scintillation effects on the transionospheric paths of propagation. Comparison is also made of the results of modeling scintillation effects utilizing HSPM and the technique of the random screen approximation.

2. Scintillation Indices for the GNSS Field on Transionospheric Paths of Propagation

[7] Along with the traditional field scintillation parameters such as the scintillation indices S_4 and σ_ϕ which characterize the intensity and phase fluctuations, other statistical moments, or their parameters, should also be used to describe the properties of the field subject to the effects of the ionospheric electron density fluctuations. Recently, *Carrano and Groves* [2010] experimentally studied time decorrelation of the intensity of the field fluctuations, the spectral index of the phase fluctuations and other parameters of the fluctuations of the field propagated through the fluctuating ionosphere. *Humphreys et al.* [2010a, 2010b] analyzed the time correlation function of the random complex amplitude of the field through the ionosphere utilizing their empirical signal model (not based on a physical scintillation propagation model). Both, in particular, studied the effects in order to understand whether or not rapid phase changes, occurring along with the deep amplitude fading, lead to the effects of cycle slips, which, in turn, may result in phase lock loss in the receiver and in order to predict the cycle slipping rates. In this section the results of our analysis of various parameters of the field scintillations (including the time correlation properties of the field) for transionospheric paths of propagation will be discussed on the basis of our physically based scintillation propagation model HSPM.

[8] A model of the transionospheric oblique channel of propagation was chosen for the analysis, which has a realistic value of the TEC of the background ionosphere. Varying the characteristic parameters of the ionospheric electron density fluctuations (e.g., the outer scales l_ε of random inhomogeneities and the variance of the fractional electron density fluctuations, σ_N^2) the effects of propagation typical for both the cases of weak and strong scintillation were produced. In modeling the ionosphere, a background ionosphere of 90 TEC units was used. For the stochastic ionosphere component, the model of the inverse power law anisotropic spectrum of the ionospheric electron density fluctuations with a spectral index of 3.7 was employed and the cross-field outer scale of fluctuations was taken to be 5 km and the aspect ratio 20. In order to provide both regimes of weak and strong scintillation of the transionospheric signal, the RMS of the fractional electron density was changed from very small values up to about 0.1 (10%) which for this maximum value and for the chosen TEC and the field-aligned and cross-field outer scale of the ionospheric random inhomogeneities yielded an S_4 value of the order of unity. Finally, the model of "frozen drift" of the random inhomogeneities of the ionosphere was utilized with a velocity of 100 m/s in the direction orthogonal to the direction of propagation.

2.1. Time Correlation Radii

[9] In Figure 1 the dependences of the scintillation index S_4 calculated using HSPM on the physical random screen (red curve), which was introduced below the ionosphere as described by *Gherm et al.* [2005], and on the Earth's surface (blue curve) are given against σ_N^2. As can be seen, for all the values of the parameters, only the case of weak, or moderate scintillation results on the screen (in accord with HSPM) but, on the Earth's surface, the scintillation index S_4 reaches the value of unity and can even exceed this value for strong and very strong scintillation conditions.

[10] For the same parameters of the scintillation propagation problem, the time correlation radii of the complex amplitude of the random field on the Earth's surface (red curve) and the field's intensity (blue curve) were calculated as a function of S_4 employing the HSPM. In the calculation, the "frozen drift" model of the random inhomogeneities of the ionosphere was employed. The results of modeling are shown in Figure 2. As far as the correlation time of the field's complex amplitude is concerned (red curve), it rapidly decreases as the scintillation severity increases. By contrast the intensity correlation time stays almost constant over a wide range of values of S_4. When S_4 approaches the value of unity, there is a "hint" (see blue curve) of a

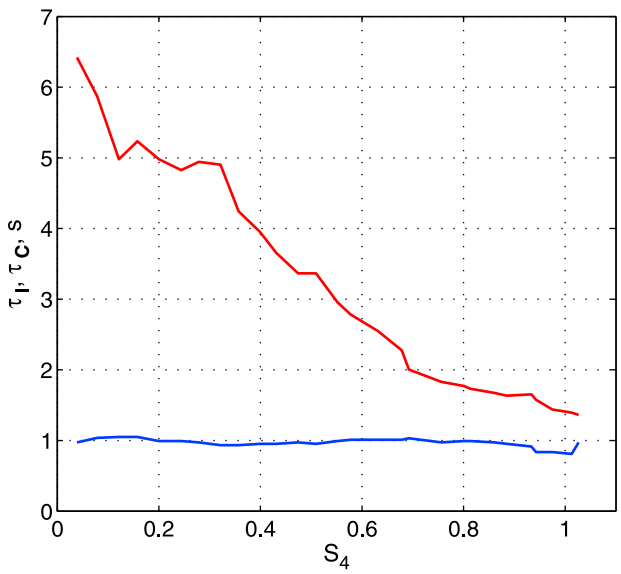

Figure 2. Time correlation radius of the complex field τ_I (red) and the field intensity τ_C (blue) in seconds.

reduction of the time correlation radius of the field intensity fluctuations. The rigorous description of a significantly reduced correlation time of the intensity lies beyond the range of validity of the HSPM. This will be the subject of an additional paper, devoted to a consideration of the case where the regime of strong scintillation arises inside the inhomogeneous ionospheric layer. For such conditions statistical focusing and the fully saturated regime of propagation may well occur on the Earth's surface.

[11] These results can be compared with the experimental observations presented by *Carrano and Groves* [2010]. In their Figure 19, they show a scatterplot of S_4 versus τ_I where it can be seen that for moderate to large values of τ_I, there is a wide range of corresponding S_4 values. This indicates that the rate of fading and depth of fading are relatively independent.

2.2. Spectral Indices of Phase and Amplitude Fluctuations

[12] Figure 3 shows the dependence of the spectral index (slope of the PSD) of the field phase and log amplitude fluctuations on S_4 derived for the same conditions of propagation as described above. Spectral indices (slope of the PSDs) of the frequency spectra of fluctuations of the phase and amplitude are plotted against S_4. These are estimated using a linear least squares fit of the high-frequency tail of the spectra, in a logarithmic scale, over the frequency range above 1 Hz. When the severity of scintillation increases, the spectral index of the phase fluctuations tends to 2. This is as expected from experimental observations [*Carrano and Groves*, 2010] and from theory as *Rino and Owen* [1980] show that for strong scatter, the rapid phase transitions caused by diffraction tend to drive the phase spectral index to that for a discontinuous process, namely, 2.0.

[13] In Figure 4, the plots of the frequency spectra of amplitude and phase fluctuations are presented for two limiting cases of weak scintillation with S_4 = 0.21 (Figure 4, left) and fairly strong scintillation with S_4 = 1.03 (Figure 4, right). As can be seen for the case of weak scintillation (Figure 4, left), both spectra of phase and log amplitude fluctuations have the same high-frequency asymptote. In the case of strong scintillation (Figure 4, right), however, the curves are separated at the high-frequency tail and have a shallower slope (spectral index) than in the case of weak scintillation.

3. Statistics of the Cycle Slips of the GNSS Field on Transionospheric Paths of Propagation

[14] Employing the HSPM to properly account for the diffraction of the field on random ionospheric inhomogeneities, it was shown by *Gherm et al.* [2011a, 2011b] and *Zernov et al.* [2011] how the occurrence of rapid phase changes associated with the deep fading may or may not lead to the accumulation of full cycles in the phase of a signal. It was shown, in particular, that once S_4 exceeds 0.6–0.7, the $2\pi M$ radians accumulated cycles are likely to appear along with rapid phase changes. It was also shown that for the same conditions of propagation, the effects of the cycle accumulation may be different at different frequencies. All together this can contribute to the increase of the range error in the dual-frequency phase method as well as the reduction of the cross-correlation coefficient of the field phases between the two frequencies.

[15] The statistics of the cycle slips of GNSS signals is of importance for different applications, in particular, for the design of receivers for GNSS signals. The investigation of this sort of statistics was performed by *Seo et al.* [2008] on the basis of the analysis of the appropriate experimental data. It is mentioned by a number of authors [e.g., *Humphreys et al.*, 2010a, 2010b; *Carrano and Groves*, 2010] that to develop the cycle slip prediction model, the statistics of S_4 are not sufficient. At high values of S_4 the cycle slipping statistics can be considered to be further specified by some other additional statistical indices, e.g., τ_I. τ_C. Here, to obtain the statistics of cycle slips (canonical fading) HSPM

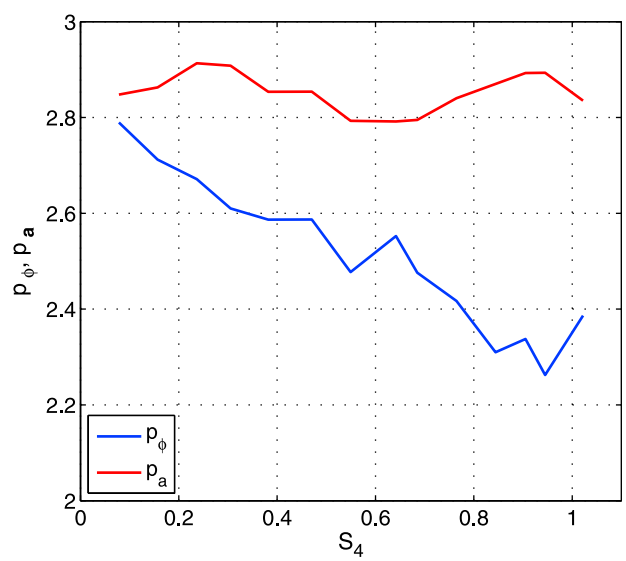

Figure 3. Spectral indices (slope of PSDs) of the phase, p_ϕ (blue), and amplitude, p_a, fluctuations, as a function of the severity of fluctuations as measured by S_4.

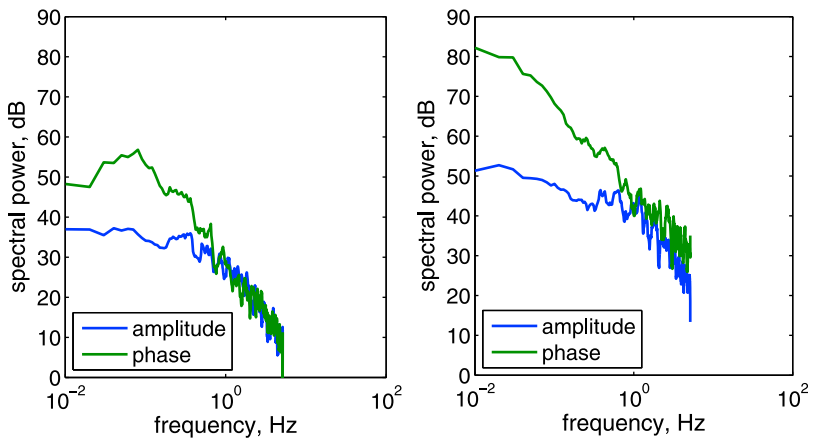

Figure 4. Frequency spectra of the field phase and amplitude fluctuations (p_ϕ, p_a) for the case of (left) weak (S_4 = 0.21) and (right) strong (S_4 = 1.03) scintillation at 1.5754 GHz.

was used. In the analysis procedure, a large number of time series of the field phase and amplitude fluctuations were generated (120 simulation runs for every given value of the RMS of the fractional electron density fluctuations of the ionosphere, σ_N, each 400 s in length) and the intervals of time were selected for which the field amplitude was smaller than a given threshold (specified as −10 dB). The intervals where, along with the deep amplitude fading of the field, fast phase changes of the order of half a cycle, or greater occurred, were classified as "canonical fading," or phase slips. The number of cases where the phase slips occurred was counted and the estimates of the mean time between the slips, Ts, were obtained as the full time of the simulation divided by the number of slips. The dependence of these events on the severity of scintillation, given by S_4, is presented in Figure 5. As can be seen, the effects of the canonical fading (cycle slips) becomes more frequent as the severity of scintillation increases. Figure 6 demonstrates possible behaviors of the random phasor of the signal in the condition of the deep fading when the fast phase changes also occur. The two panels show how the deep fading may result in a half-cycle slip (Figure 6, left) or an approximately full cycle slip (Figure 6, right).

[16] Here we should emphasize that we have, in effect, calculated the cycle slips that occur at the receiver antenna from the propagation process and we do not additionally predict the effect of the receiver on the signal in which PLL loss of lock can occur. This has been studied by other authors. For example, *Moraes et al.* [2012] study cycle slips solely on the basis of amplitude fluctuation measurements. They use the formula, introduced by *Humphreys et al.* [2010a] to predict the possible occurrence and statistics of cycle slips depending on the severity of the fluctuations which are likely to be observed by a receiver at the PLL output, employing solely the results of the amplitude scintillation measurements. By contrast what has been obtained with our physical model, and presented here, is what the real field looks like at the input to the receiver at the point of the receiver location so that in the sense of a field treatment in terms of amplitude and phase, the phase may have what is termed by *Humphreys et al.* [2010a] canonical fading. Thus strictly speaking, the graph in Figure 5 presents the statistics of the *field's* canonical fading occurrences as a function of the severity of scintillation.

4. Comparison of the HSPM and the Effective Phase Screen Approximation to Model the GNSS Field Scintillation on Transionospheric Paths of Propagation

[17] The equivalent phase screen technique is widely used in order to give the interpretation of different experimental data of scintillation (see, e.g., *Rino* [1979] and *Rino and Owen* [1980] and many other papers employing this method). According to this technique, as the first step, the fluctuating part of the phase of the field which has traversed the ionosphere with given parameters of both the background ionosphere and the electron density fluctuations, is calculated as the integral along the line of sight connecting

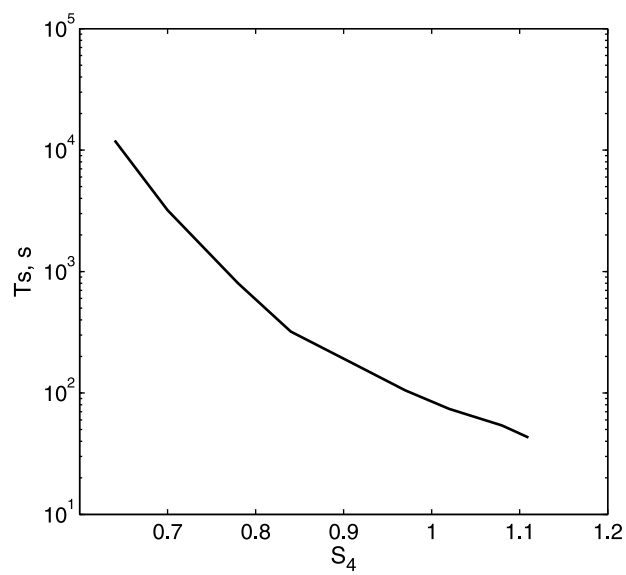

Figure 5. The mean time interval between the occurrence of cycles slips, Ts, in seconds as a function of the severity of the scintillation, given by S_4.

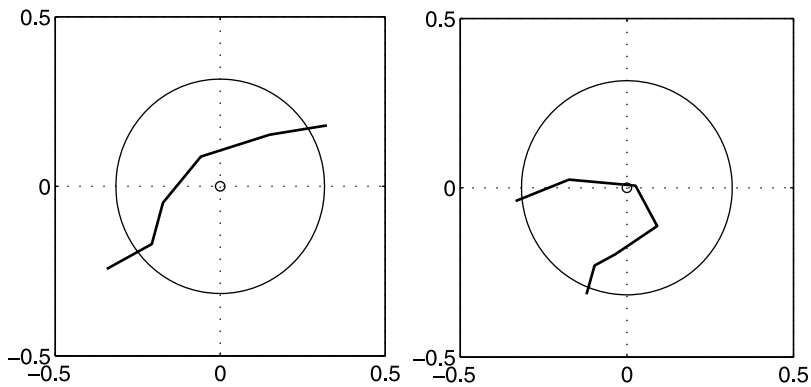

Figure 6. Example random walks of the full field phasor showing the types of cycle slips: (left) half a cycle slip and (right) a cycle slip. Circles correspond to fading of 10 dB.

the satellite and the point of observation. After the random phase on the screen is described, the screen is placed at a height above the Earth's surface, which is normally around the height of the maximum of the ionospheric F2 layer. Once the height of the screen has been specified, it may be the case, however, that for the chosen parameters, the phase screen model does not provide good agreement with the experimental data (or with calculated results using another independent method). To achieve a fit, it appears necessary to make changes to the model parameters, e.g., the height of the screen, or, alternatively, the parameters of the random phase on the screen. This can be considered to be a limitation of the phase screen technique to self-consistently describe the scintillation effect. By contrast, the HSPM, since based on solving the appropriate equations governing the propagation process, provides (within its range of validity) self-consistent descriptions of the scintillation effects once the physical conditions of propagation have been specified. Below we provide a comparison of the results of modeling scintillation effects obtained utilizing both the phase screen technique and the HSPM. Calculations have been performed for the same parameters of the stochastic channel of propagation as given in section 2.

[18] In Tables 1 and 2 scintillation indices are presented calculated by the HSPM and the random screen technique for the conditions of (1) weak and (2) strong scintillation. The scintillation index S_4, spectral indices for the frequency spectra of the field log amplitude p_a and phase p_ϕ fluctuations, time correlation radii of the intensity τ_1 and complex field τ_c have been compared. As is seen from Tables 1 and 2, some parameters appear different when calculated by HSPM from those determined by the random phase screen technique. In particular, once the results obtained using HSPM are accepted as the reference, the height of the phase screen in the conditions of weak scintillation should be chosen as 600 km to provide good agreement to those of HSPM for the majority of indices. However, even with this adjustment, the values of the time correlation radius of the complex field are rather different. In the case of strong scintillation, the height of the random screen of 600 km only provides good agreement for S_4 values while other indices are a little different. Finally, as seen from Tables 1 and 2, the height of the screen of 350 km does not provide agreement with the HSPM for S_4 and τ_c in the weak scintillation case and for S_4, p_a and p_ϕ in the case of strong scintillation.

5. Conclusions

[19] An updated version of the HSPM which was previously developed [*Gherm et al.*, 2011a, 2011b] has been employed further to investigate a number of the effects of scintillation on GNSS signals for transionospheric paths of propagation, specifically for the case of strong scintillation. A number of parameters including spectral indices and other statistical moments of the scintillation of the field have been studied as a function of the severity of the signal fluctuations.

[20] First, an approximately linear relation was found between the S4 index and the variance of the electron density variations. The dependence of the correlation time of the complex amplitude of the field on S_4 was then determined and was found to rapidly decrease as the scintillation severity increased but, by contrast, the intensity correlation time stayed almost constant over a wide range of values of S_4 except for when S_4 approached the value of unity when there was some evidence of a reduction. This will be the subject of an additional paper, devoted to a consideration of

Table 1. Comparison of the Results Generated by HSPM and the Phase Screen Approximation: Weak Scintillation[a]

	Hybrid Method	Phase Screen H = 350 km	Phase Screen H = 600 km
S_4	0.21 ± 0.003	0.17 ± 0.003	0.22 ± 0.006
p_a	2.9 ± 0.2	2.9 ± 0.1	2.9 ± 0.2
p_φ	2.7 ± 0.2	2.8 ± 0.2	2.8 ± 0.1
τ_I	1.0 ± 0.1	1.0 ± 0.1	1.2 ± 0.2
τ_C	6.1 ± 1.7	4.3 ± 1.4	4.5 ± 1.3

[a]RMS of the fractional electron density is 0.013.

Table 2. Comparison of the Results Generated by HSPM and the Phase Screen Approximation: Strong Scintillation[a]

	Hybrid Method	Phase Screen H = 350 km	Phase Screen H = 600 km
S_4	1.03 ± 0.01	0.85 ± 0.03	1.0 ± 0.04
p_a	2.6 ± 0.2	3.0 ± 0.2	3.0 ± 0.2
p_φ	2.3 ± 0.2	2.6 ± 0.2	2.5 ± 0.2
τ_I	0.85 ± 0.1	0.8 ± 0.1	0.9 ± 0.1
τ_C	1.2 ± 0.1	1.3 ± 0.3	1.3 ± 0.2

[a]RMS of the fractional electron density is 0.07.

the case where the regime of strong scintillation arises inside the inhomogeneous ionospheric layer. For such conditions statistical focusing and the fully saturated regime of propagation may well occur on the Earth's surface.

[21] The dependence of the spectral indices of both phase and log amplitude on S_4 was also determined and the spectral index of the phase fluctuations was found to tend to 2 as expected from both experiment and theory. It was also found that in the conditions of strong scintillation, when deep amplitude fades frequently occur, this is likely to be accompanied by fast phase changes, which may lead to full $2\pi M$ radians (where M is a positive, or negative integer) phase accumulation. The probability of this effect was investigated for the conditions of strong scintillation and the mean time between cycle slips was found to decrease significantly with increasing S_4 for large S_4 values.

[22] A comparison was also presented between calculated results of S_4, spectral indices of phase and amplitude and the correlation radii of the complex field and field intensity utilizing both the HPSM and equivalent phase screen model for both weak and strong scintillation conditions. This showed the differences that can occur between calculations using the two methods and which were shown to depend on the equivalent phase screen height. This can be considered to be a limitation of the phase screen technique to self-consistently describe the scintillation effect.

[23] Finally, the ability of the simulator to model the input to a GNSS receiver during even strong scintillation conditions makes it very useful for investigating the response to these conditions of different GNSS receivers both present or postulated (the latter with the use of a software receiver) to enable optimum hardware and firmware receiver modifications for scintillation mitigation to be determined and validated.

References

Carrano, C. S., and K. M. Groves (2010), Temporal decorrelation of GPS satellite signals due to multiple scattering from ionospheric irregularities, paper presented at the 23rd International Technical Meeting, Satell. Div., Inst. of Navig., Portland, Oreg., 20–24 Sept.

Gherm, V. E., N. N. Zernov, S. M. Radichella, and H. J. Strangeways (2000), Propagation model for signal fluctuations on transionospheric radio links, *Radio Sci.*, *35*(5), 1221–1232, doi:10.1029/1999RS002301.

Gherm, V. E., N. N. Zernov, and H. J. Strangeways (2005), Propagation model for transionospheric fluctuational paths of propagation: Simulator of the transionospheric channel, *Radio Sci.*, *40*, RS1003, doi:10.1029/2004RS003097.

Gherm, V. E., N. N. Zernov, and H. J. Strangeways (2011a), Effects of diffraction by ionospheric electron density irregularities on the range error in GNSS dual-frequency positioning and phase decorrelation, *Radio Sci.*, *46*, RS3002, doi:10.1029/2010RS004624.

Gherm, V. E., N. N. Zernov, and H. J. Strangeways (2011b), Phase de-correlation due to the field diffraction on stochastic ionospheric irregularities in spaced-frequency transionospheric measurements, paper presented at 13th International Ionospheric Effects Symposium, Off. of Nav. Res., Alexandria, Va., 17–19 May.

Humphreys, T. E., M. L. Psiaki, and P. M. Kintner Jr. (2010a), Modeling the effects of ionospheric scintillation on GPS carrier phase tracking, *IEEE Trans. Aerosp. Electron. Syst.*, *46*(4), 1624–1637, doi:10.1109/TAES.2010.5595583.

Humphreys, T. E., M. L. Psiaki, B. M. Ledvina, A. P. Cerruti, and P. M. Kintner Jr. (2010b), A data-driven testbed for evaluating GPS carrier tracking loops in the ionospheric scintillation, *IEEE Trans. Aerosp. Electron. Syst.*, *46*(4), 1609–1623, doi:10.1109/TAES.2010.5595582.

Maurits, S. A., V. E. Gherm, N. N. Zernov, and H. J. Strangeways (2008), Modeling of scintillation effects on high-latitude transionospheric paths using ionospheric model (UAF EPPIM) for background electron density specifications, *Radio Sci.*, *43*, RS4001, doi:10.1029/2006RS003539.

Moraes, A. O., F. S. Rodrigues, W. J. Perrella, and E. R. de Paula (2012), Characteristics of low-latitude GPS amplitude scintillation measured during solar maximum conditions and implications for receiver performance, *Surv. Geophys.*, doi:10.1007/s10712-011-9161-z, in press.

Rino, C. L. (1979), A power law phase screen model for ionospheric scintillation: 1. Weak scatter, *Radio Sci*, *14*, 1135–1145.

Rino, C. L., and J. Owen (1980), The time structure of transionospheric radio wave scintillation, *Radio Sci.*, *15*(3), 479–489, doi:10.1029/RS015i003p00479.

Seo, J., T. Walter, T.-Y. Chio, and P. Enge (2008), Characteristics of deep GPS signal fading due to ionospheric scintillation for aviation receiver design, paper presented at 12th International Ionospheric Effects Symposium, Off. of Nav. Res., Alexandria, Va., 13–15 May.

Zernov, N. N., V. E. Gherm, and H. J. Strangeways (2009), On the effects of scintillation of low-latitude bubbles on transionospheric paths of propagation, *Radio Sci.*, *44*, RS0A14, doi:10.1029/2008RS004074.

Zernov, N. N., V. E. Gherm, and H. J. Strangeways (2011), Effects of cycle slips on the range error in dual-frequency GNSS measurements, paper presented at 13th International Ionospheric Effects Symposium, Off. of Nav. Res., Alexandria, Va., 17–19 May.

V. E. Gherm and N. N. Zernov, Department of Radio Physics, University of St. Petersburg, Ulyanovskaya 1, 198504 St. Petersburg, Russia. (gherm@paloma.spbu.ru; zernov@paloma.spbu.ru)

H. J. Strangeways, School of Electrical, Electronic and Computer Engineering, University of Newcastle, Newcastle upon Tyne NE1 7RU, UK. (h.j.strangeways@ncl.ac.uk)